Kinetics of chromate reduction by nano zero valent iron incorporated in a porous matrix

Aik.Toli[1*], L. Karavanas[1] , Ch. Mystrioti[1], N. Papassiopi[1]

1Sch. of Mining and Metallurgical Eng., National Technical University of Athens, 15780, Greece

*Corresponding author: E-mail: katerinatoli@metal.ntua.gr, Tel 2107722388, Fax +30 210 7722129

Abstract

Incorporation of nanozero valent iron (nZVI) in a porous matrix is an innovative technology for the treatment of contaminated waters. Aim of the technology is to exploit the high reactivity of nZVI towards a wide spectrum of contaminants, avoiding important handling problems which arise when bare nZVI suspensions are used. In this study nZVI was incorporated in the matrix of a cation-exchange resin (Amberlyst 15), by applying a green synthesis procedure, and the composite material was used for the removal of Cr(VI) from aqueous solutions. Reduction kinetics was studied by conducting batch tests. The main investigated parameters were the particle size of nZVI loaded resin beads (R-nFe), the concentration of Cr(VI) and the amount of R-nFe per volume of solution.

A model was developed to describe the reduction kinetics, taking into consideration two interrelated processes: (a) the diffusion of contaminant inside the network of pores and (b) the chemical reaction between the contaminant and iron nanoparticles which are homogenously dispersed inside the porous beads. The effective diffusion coefficient, De, and the kinetic constant, k, were initially determined by fitting the model equations to an initial set of experimental data, and then were successfully used to predict the kinetics under different experimental conditions.

Keywords: chromate, iron nanoparticles, Amberlyst 15, reduction kinetics, intraparticle diffusion.

1. Introduction

Various metals in the zero oxidation state, such as Fe^0, Zn^0, Sn^0, Ni^0, Mg^0 and Al^0, can be effective for the remediation of polluted groundwater (Powell *et al*., 1998). Elemental iron (Fe^0) is the most commonly used because it combines many advantages in comparison to other alternatives, such as high efficiency, low cost, widespread availability and environmental compatibility. Zerovalent iron nanoparticles in nanoscale (nZVI) are typically less than 100 nm in diameter, with a spherical shape, and they form chain-type agglomerates. The surface activity, the catalytic ability and the mechanical properties can be increased by 10 to 100 times in comparison with microscale metallic iron (O'Carroll *et al*., 2013).

In spite of nano ZVI efficiency for the removal of a wide spectrum of contaminants, both organic and inorganic, there are some drawbacks which limit the applicability of this technology, such as difficulties in effectively separating the nanoiron from the purified aqueous phase and concerns about possible negative effects on the ecosystem in case of uncontrolled release in the aquatic environment. To overcome these problems, two alternatives have been investigated: (i) fixation of nZVI on the surface of an appropriate material and (ii) incorporation of nZVI in the matrix of a porous material. Various natural clay minerals, like bentonite, kaolinite, zeolite, and polygorskite, have been proved to be good carriers for the surface deposition of nZVI. With this technology the resulting composite material can be easily separated from the aqueous medium by conventional sedimentation or filtration processes. When nZVI is incorporated in a porous matrix, the resulting composite material is usually of granular form and can be used in packed bed installations, thus avoiding the sedimentation/ filtration steps for the separation of aqueous stream. Porous matrices which have been tested for the encapsulation of nZVI include pumice grains, ion exchange resins, chitosan beads, granular activated carbon, etc. (Cumbal *et al*., 2003; Tseng *et al*., 2011;) (Liu *et al*., 2010). The effectiveness of composite materials with encapsulated nZVI was evaluated for the removal of heavy metals, chromate anions, nitrates, etc.

In previous studies we have presented the results of our research involving the incorporation of nZVI in the matrix of cation exchange resins and the use of these composite materials for the treatment of Cr(VI) contaminated waters (Toli 2016a, b). It was found that the kinetics of chromate reduction was first order with respect to Cr(VI) and to the amount of embedded nZVI, as described by equation (1):

$$-\frac{dC_A}{dt} = k_{2L,obs} \cdot C_{BL} \cdot C_A \qquad (1)$$

where C_A is the concentration of chromate in the aqueous phase and C_{BL} the concentration of embedded nZVI, expressed as mmole per liter of aqueous solution. The value of $k_{2L,obs}$ constant was found to range between $0.5 \cdot 10^{-3}$-$8.0 \cdot 10^{-3}$ min^{-1} per mM of nZVI. The kinetics of Cr(VI) reduction using bare nZVI suspensions is much faster compared to the kinetics with embedded nZVI. Namely, the second order kinetic constant was estimated to be approximately 1000 times higher, i.e. 0.5 min^{-1} per·mM of nZVI (Toli *et al*., 2016). The slower kinetics in the case of embedded nZVI was attributed to the effect of

intraparticle diffusion, i.e. the resistance for the transfer of chromates from the bulk of aqueous phase to the incorporated nZVI, through the pore network of the host material. Although the importance of intraparticle diffusion was recognized, there was no effort till now to describe the kinetics with models incorporating the simultaneous effect of intraparticle diffusion and chemical reaction. Such types of models have been primarily developed to describe catalytic reactions that take place using solid porous catalysts (Levenspiel, 1962, Froment *et al*., 2011).

In the present study nZVI was incorporated in the matrix of a cation-exchange resin (Amberlyst 15), by applying a green synthesis procedure, based on the use of plant polyphenols for the reduction of Fe(III) to the elemental state. The composite material was used for the removal of Cr(VI) from aqueous solutions. Reduction kinetics was studied by conducting batch tests. The main investigated parameters were the particle size of nZVI loaded resin beads (R-nFe), the concentration of Cr(VI) and the amount of R-nFe per unit volume of solution.

A model was developed to describe the reduction kinetics, taking into consideration the two interrelated processes, i.e. intraparticle diffusion and chemical reaction. The effective diffusion coefficient, De, and the intrinsic kinetic constant, k, were initially determined by fitting the model equations to an initial set of experimental data, and then were used to predict the kinetics under different experimental conditions.

2. Materials and Methods

2.1 Materials

All chemical reagents were of analytical reagent grade. Potassium dichromate ($K_2Cr_2O_7$) and iron chloride ($FeCl_3.6H_2O$) were purchased from Mallinckrodt Chemical Works, USA and Alfa Aesar, Germany, respectively. Sodium chloride was obtained from Merck, Germany. Also commercially available dry leaves of green tea (Twinings of London) were used as sources of polyphenols. The resin Amberlyst 15 H^{+} form is macro reticular polystyrene based ion exchange resin with strongly acidic sulfonic groups and was purchased from Sigma Aldrich, China. The porosity was equal to 31.9% and the mean size of pores was determined by BET analysis to be equal to 38.4 nm. Measured specific surface was 33 m^2/g.

2.2 Incorporation of nZVI in the resin beads

The commercial resin Amberlyst 15 had a relatively wide particle size distribution. Namely, 13% (per wet weight) of beads had diameter size in the range 1.0-0.85 mm, 62% in the range 0.5-0.7 mm and 23% belonged to the range 0.3-0.5 mm. The bulk resin was separated in the above three fractions, in order to obtain working samples with homogenous particle size.

The incorporation of nZVI in the resin beads and the ground sample was carried out at two steps. The first step involved the adsorption of Fe(III) cations in the resin and the second step the reduction of adsorbed Fe(III) to the elemental state Fe(0) by mixing the iron laded resin with green tea extract. The resin treated with GT is denoted as

R-nFe in the following text. The detailed synthesis procedure is given in Toli *et al*. (2016a, b). The amount of nanoiron embedded in the beads was equal to 0.50±0.02 mmole per gram of wet resin. SEM/EDS analyses were carried out on several cut sections of the resin beads and indicated that the iron nanoparticles were homogenously distributed inside the resin matrix (Toli 2016a, b).

2.3 Investigation of Cr(VI) reduction kinetics by batch experiments

An initial set of kinetic experiments were carried out to investigate the effect of particle size. The used R-nFe samples had a mean particle diameter equal to 462.5 μm, 388 μm and 300 μm. The tests were conducted mixing 2 g of R-nFe with 100 mL of a solution containing 20 mg/L Cr(VI).

The effect of initial Cr(VI) concentration on the rate of Cr(VI) removal was investigated in the range of 5-20 mg/L. The experiments were carried out mixing the aqueous solution with 20 g/L R-nFe. A third series of tests was carried out to study the effect of resin dose. An aqueous solution containing 20 mg/L Cr(VI) was mixed with R-nFe at variable doses, i.e. 20, 40 and 60 grams R-nFe per liter.

The experiments were carried out using shaking flasks which were placed in an orbital agitator. The suspensions were agitated at 200 rpm for 120 min and the temperature was kept constant at 25°C. Samples were taken at 30, 60, 90 and 120 min and analyzed for Cr(VI). All experiments were conducted in duplicate.

2.3 Mathematical model of intraparticle diffusion with chemical reaction

Intraparticle diffusion with simultaneous reaction has been described for catalytic reactions, where a reactant A in the fluid phase diffuses through the pores of a solid catalyst and the reaction takes place on the pore walls (Levenspiel, 1962, Froment *et al*., 2011). In our case the reaction takes place between hexavalent chromium (the fluid reactant A) and iron nanoparticles (reactant B), which are homogenously dispersed inside the pores. Contrary to the case of catalytic reactions, in the examined system reactant B is consumed. According to the stoichiometry of reaction (2), one mole of Cr(VI) is reduced by one mole of elemental iron:

$$HCrO_4^- + Fe^0 + 7H^+ \rightarrow Cr^{+3} + Fe^{+3} + 4H_2O \qquad (2)$$
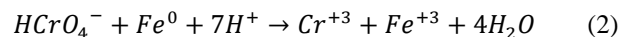
When reaction occurs inside the pores simultaneously with diffusion, the process is not a strictly consecutive one and both phenomena must be considered together. For diffusion through a spherical particle and a first-order reaction, the transient continuity equation for *A* can be written according to equation (3):

$$\frac{\partial^2 C_A}{\partial r_p^2} + \frac{2}{r_p}\frac{\partial C_A}{\partial r_p} - \frac{k_{1p}}{D_e}C_A = \frac{\varphi}{D_e}\frac{\partial C_A}{\partial t} \qquad (3)$$

where r_p: is the radial distance from the center of the particle (m), D_e: is the effective diffusion coefficient through the porous particle (m^2/s), k_{1p}: is the kinetic constant for a first order reaction, when the rate is

expressed using as basis the volume of resin particle (s^{-1}) and φ: is the porosity.

A first criterion to evaluate how much the reaction rate is lowered because of the resistance to pore diffusion is the value of the dimensionless parameter M_T, known as Thiele modulus (Levenspiel, 1962):

$$M_T = \frac{R}{3}\sqrt{\frac{k_{1p}}{D_e}} \qquad (4)$$

When M_T is small, or $M_T < 0.4$, pore diffusion offers negligible resistance. For large M_T, or $M_T > 4$, diffusion strongly influences the rate of reaction.

The spatial variable r_p can be replaced with the distance x from the surface of the particle towards the center of the sphere

$$x = R - r_p \qquad (5)$$
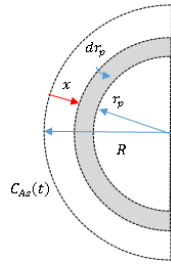
Figure 1. Schematic representation of the resin bead

Eq. (3) becomes:

$$\frac{\partial^2 C_A}{\partial x^2} - \frac{2}{R-x}\frac{\partial C_A}{\partial x} - \frac{k_{1p}}{D_e}C_A = \frac{\varphi}{D_e}\frac{\partial C_A}{\partial t} \qquad (6)$$

For the definition of boundary conditions we consider that at $x = 0$ (the outer surface of particle), the concentration of solute A (chromates) is equal to C_{AS}. At the center of particle, the gradient of A concentration is equal to zero. These conditions can be written as:

$\forall$ t, $\quad x = 0 \ (r_p = R)$, $\ C_A = C_{AS}(t)$ $\quad$ and $\quad$ $x = R \ (r_p = 0)$, $\frac{\partial C_A}{\partial x} = 0$

The following initial conditions also apply:

$\forall\ x > 0$, $\qquad t = 0,\ C_A = 0$
$x = 0$, $\qquad t = 0,\ C_A = C_{AS0}$

The resistancefor the external mass transfer of A from the bulk of the liquid to the outer surface of particle is considered negligible. For this reason the concentration of solute A in the outer surface of particle, $C_{AS}(t)$, is taken equal to the concentration in the bulk of aqueous solution.

In the examined system the term k_{1p} is not constant because depends on the concentration of nZVI in the porous particle:

$$k_{1p} = k_{2p} \cdot C_B \rho_a \qquad (7)$$

k_{2p} : is the 2nd order kinetic constant, when the rate is expressed per unit volume of resin particle (mol^{-1}·m^3·s^{-1}), C_B: is the concentration of B (nZVI) per unit mass of resin

(mol·kg^{-1}) and ρ_a: is the particle density of resin beads (kg·m^{-3}).

The partial differential equation was solved numerically using the Madonna Berkeley software. For every time instant, t_j, calculations were carried out for the successive radial positions x_i, inside the spherical particle. The first and second spatial partial derivatives were calculated using the methode of central difference (equ 8 and 9):

$$\left(\frac{\partial C_A}{\partial x}\right)_{i,j} = \frac{C_{A_{i+1,j}} - C_{A_{i-1,j}}}{2\Delta x} \qquad (8)$$

$$\left(\frac{\partial^2 C_A}{\partial x^2}\right)_{i,j} = \frac{C_{A_{i+1,j}} - 2C_{A_{i,j}} + C_{A_{i-1,j}}}{\Delta x^2} \qquad (9)$$

The temporal derivative $\left(\frac{\partial C_A}{\partial t}\right)_{i,j}$ was calculated from equation (6). Integration versus time was carried out using the Runge-Kutta 4 method.

The progress of reaction $\xi_{i,j+1}$ (mol of A and B that have reacted) at time t_{j+1} was calculated for each radial position x_i, and for the entire population of resin particles, according to equations (10) and (11):

$$\left(\frac{d\xi}{dt}\right)_{i,j} = r_{i,j} \cdot \Delta V_i \cdot n_B \qquad (10)$$

$$\xi_{i,j+1} = \xi_{i,j} + \left(\frac{d\xi}{dt}\right)_{i,j}\Delta t \qquad (11)$$

where: ΔV_i:volume of the spherical shell at the radial position x_i with thickness Δx (m^3), $r_{i,j}$: reaction rate at x_i and t_j(mol·m^3·s^{-1}), and n_B: total number of resin particles.

$$r_{i,j} = k_{2p} \cdot C_{B(i,j)}\rho_a \cdot C_{A_{i,j}} \qquad (12)$$

$$\Delta V_i = 4\pi(R - x_i)^2 \Delta x \qquad (13)$$

$$n_B = \frac{N_{B0}}{\frac{4}{3}\pi R^3 \rho_a C_{B0}} \qquad (14)$$

$$N_{B0} = C_{B0}M_R \qquad (15)$$

$$C_{B(i,j)} = C_{B0} - \frac{\xi_{i,j}}{n_B \rho_a \Delta V_i} \qquad (16)$$

N_{B0}: initial amount of nZVI (mol), C_{B0}: initial homogenous concentration of nZVI per unit mass of resin particles (mol·kg^{-1}), and $C_{B(i,j)}$: concentration of nZVI at radial position x_i and time t_j (mol·kg^{-1}).

The total molar mass of A that has remained in the system at time t_j is calculated taking into consideration the progress of reaction at all radial positions x_i (equ 17):

$$N_{Aj} = N_{A0} - \sum_{i=1}^{I} \xi_{ij} \qquad (17)$$

where N_{A0}: initial amount of Cr(VI) (mol) and N_{Aj} remaining Cr(VI) at time t_j (mol). Part of the unreacted Cr(VI) is retained inside the pores of resin beads and can be calculated from equation (18):

$$N_{Apj} = n_B \sum_{i=1}^{I} C_{Aij} \Delta V_i \varphi \qquad (18)$$

The concentration of Cr(VI) in bulk solution at time t_j is thus calculated as follows:

$$C_{AS,j} = \frac{N_{Aj} - N_{Apj}}{V_L} \qquad (19)$$

The unknown parameters of the model are the intrinsic kinetic constant k_{2p} and the effective diffusivity D_e. An initial set of experimental data was used to estimate these parameters by fitting the calculated values of $C_{AS,j}$ to the experimental ones. The optimization criterion was the minimization of the root mean square error (RMSE) corresponding to the differences between individual data points in the dataset and the corresponding calculated points in the run. Missing experimental data were approximated for all time instants, t_j, by linear regression between successive available measurements.

$$RMSE = \sqrt{\frac{1}{J} \sum_{1}^{J} \left(C_{AS,j,calc} - C_{A,j,exp} \right)^2} \qquad (18)$$

3. Experimental and modeling results

3.1 Effect of resin particle size

The experimental results obtained with resin beads of different diameter are presented in Figure 2. The results indicate that the rate of Cr(VI) reduction was not affected by the size of resin beads. The measurements of duplicate tests presented a relative difference varying between 0.5 and 20% compared to the mean values. However, the mean values were very close at all sampling times for all three particle sizes. According to the classical approach, this happens when pore diffusion offers negligible resistance in comparison with the intrinsic chemical reaction. In this case the value of Thiele modulus is low, i.e. $M_T < 0.4$ (equ. 4).

The model was initially run using as adjustable parameters the Thiele modulus M_T and the intrinsic kinetic constant k_{2p}. The diffusivity parameter was calculated indirectly from equation (4). The acceptable ranges for the two parameters were set as: $0.2 < M_T < 1$ and $0.14 \cdot 10^{-4} < k_{2p} < 14 \cdot 10^{-4}$ (mol^{-1}·m^3·s^{-1}). This range of M_T was selected taking into account the negligible effect of particle size.
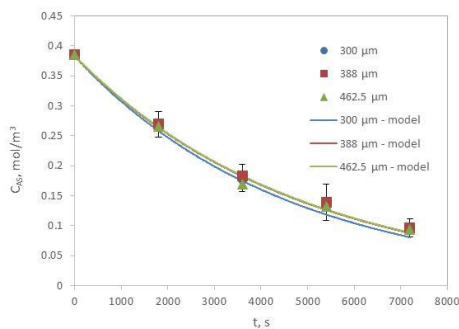
Figure 2. Reduction of Cr(VI) at different grain sizes of the resin. The bars represent the deviation of duplicate measurements

The range of the intrinsic kinetic constant k_{2p} was defined based on preliminary tests (data not shown), which were carried out with nZVI embedded on a finely ground resin sample, under conditions excluding the interference of diffusion. These experiments indicated the value of $1.4 \cdot 10^{-4}$ mol^{-1}·m^3·s^{-1} as a possible level of k_{2p}. The determined fitted values were **$M_T = 0.639$** and **$k_{2p} = 2.48 \cdot 10^{-5}$ mol^{-1}·m^3·s^{-1}**. Based on these values the effective diffusivity was calculated to be **$D_e = 7.46 \cdot 10^{-10}$ m^2/s**. According to Li *et al.* (2007) the diffusivity of chromate in free water is equal to $1.27 \ 10^{-9}$ m^2/s. The calculated D_e value is considered as a realistic approximation for Cr(VI) transfer in the porous matrix. The evolution of Cr(VI) concentration for the two other particle sizes, R=388 μm and R=300 μm was described maintaining the two parameters k_{2p} and D_e at the previously determined values, $2.48 \cdot 10^{-5}$ mol^{-1}·m^3·s^{-1} and $7.46 \cdot 10^{-10}$ m^2/s respectively. As seen in Figure 2, the model predicts a reduction kinetics which is slightly faster using the resin particles with the smallest size. However, the kinetics for all particle sizes is very close and the differences could not be distinguished experimentally. The evolution of Cr(VI) concentrations at several radial positions inside the resin particles is shown in Figure 3. As seen in figure 3a in the case of small particles (R=300 μm) the concentration of Cr(VI) is the same at all radial positions at every time. This suggests that Cr(VI) is transferred rapidly through the pores, establishing an homogenous concentration inside the whole volume of the particle. In the case of larger particles (R=462.5 μm, Figure 3b) the concentration of Cr(VI) is higher at the surface and decreases constantly moving towards the center of the particle. This suggests that diffusion is starting to influence the kinetics.

(a) R = 300 μm
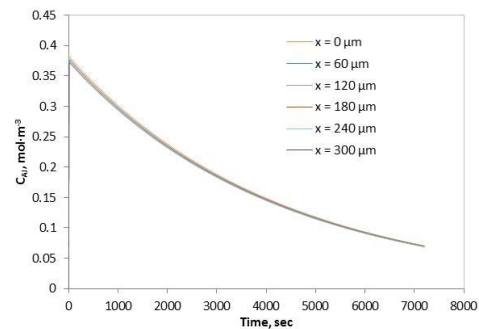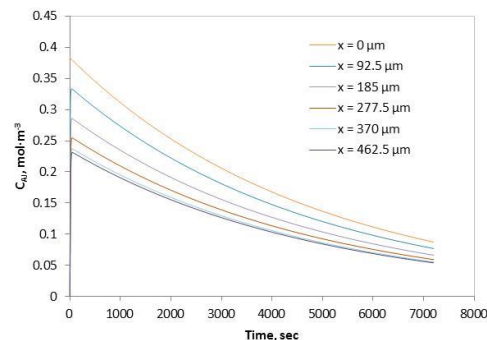
(b) R = 462.5 μm

Figure 3. Concentration of Cr(VI) at several radial positions inside the resin particles for (a) small (R=300 μm) and (b) large (R=462.5 μm) particles.

3.2 Effect of different Cr(VI) concentrations and resin doses

The effect of initial Cr(VI) concentration on Cr(VI) removal was investigated at three levels 0.096, 0.192 and 0.385 $mol\cdot m^{-3}$. The experimental data in comparison with model output are presented in Fig. 4. The results with different resin doses, i.e. 20, 40 and 60 g/L, are presented in Figure 5. For all the experiments, the model runs were carried out using the same k_{2p} and D_e parameters as previously.

The accordance between experimental and calculated values was very satisfactory. The RMSE deviation between model output and experimental data is shown in Table 1. RMSE compared to the mean value of measured concentrations in each experiment, $(C_{A,max} - C_{A,min})/2$, represents a low percentage, i.e. $< 7\%$. Another series of model runs were carried out maintaining De value constant and using k_{2p} as adjustable parameter. The fitted values of k_{2p} are also presented in Table 1. The numbers are very close with a mean value equal to $2.46\cdot10^{-5}$ and standard deviation equal $0.24\cdot10^{-5}$ $(mol^{-1}m^3\ s^{-1})$.

4. Conclusions

The reduction of Cr(VI) by resin embedded nZVI can successfully be described by a model incorporating two interrelated processes: (a) the diffusion of contaminant inside the network of pores and (b) the chemical reaction between the contaminant and embedded iron nanoparticles
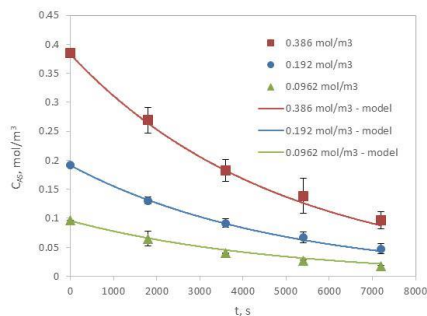
Figure 4. Time evolution of Cr(VI) at different initial Cr(VI) concentrations.
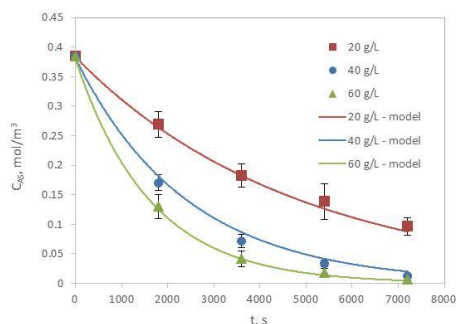
Figure 5. Time evolution of Cr(VI) at different resin doses. Experimental data and model results.

Table 1.RMSE deviation between model output and experimental data using the parameters k_{2p}= 2.48 $\cdot10^{-5}$ $(mol^{-1}\cdot m^3 \cdot s^{-1})$ and D_e =$7.46\cdot10^{-10}$ (m^2/s). Comparison with RMSE when the model is run with constant De and adjustable k_{2p}.

Particle size (μm)	Resin Dose (g R/L)	Initial Cr(VI) (mol·m⁻³)	RMSE* (mol·m⁻³)	Fitted k_{2p} ×10⁵ (mol⁻¹m³ s⁻¹) and constant D_e =0.746·10⁻⁹ m²s⁻¹	
				k_{2p}	RMSE (mol·m⁻³)
300	20	0.385	0.01028	2.11	0.00425
388	**20**	**0.385**	0.00862	2.31	0.00352
462.5	20	0.385	0.00584	2.48	0.00598
388	20	**0.0962**	0.00353	2.84	0.00162
388	20	**0.192**	0.00336	2.35	0.00168
388	**40**	0.385	0.00882	2.76	0.0089
388	**60**	0.385	0.01644	2.36	0.0140

The main parameters of the model, i.e. effective diffusivity of chromate and intrinsic kinetic constant were determined by fitting the model results to one set of experimental data and they were proved to describe with satisfactory accuracy the kinetics of Cr(VI) under different experimental conditions.

References

Cumbal, L., Greenleaf, J., Leun, D., SenGupta, A.K., 2003. Polymer supported inorganic nanoparticles: Characterization and environmental applications. React. Funct. Polym. 54, 167–180. doi:10.1016/S1381-5148(02)00192-X

Froment, G., Bischoff K., and De Wilde, J., 2011. Chemical Analysis and Reactor, 3rd edition. Wiley, Hoboken.

Levenspiel, O., 1962. Chemical Reaction Engineering, Wiley, New York.

Liu, T.Y., L. Zhao, D.S. Sun, X. Tan (2010) Entrapment of nanoscale zero-valent iron in chitosan beads for hexavalent chromium removal from wastewater, J. Hazard. Mater., 184, pp. 724–730

O'Carroll, D., Sleep, B., Krol, M., Boparai, H., Kocur, C., 2013. Nanoscale zero valent iron and bimetallic particles for contaminated site remediation. Adv. Water Resour. 51, 104–122. doi:10.1016/j.advwatres.2012.02.005

Powell, R.M., Puls, R.W., Blowes, D.W., Vogan, J.L., Gillham, R.W., Powell, P.D., Schultz, D., Sivavee, T., Landis, R., 1998. Permeable Reactive Barrier Technologies for Contaminant Remediation. Epa/600/R-98/125 113. doi:EPA/600/R-98/125

Thiele, E. W., (1939) Relation between Catalytic Activity and Size of Particle Ind. Eng. Chem., 31, 916-920.

Toli, A., Chalastara, K., Mystrioti, C., Xenidis, A., Papassiopi, N., 2016. Incorporation of zero valent iron nanoparticles in the matrix of cationic resin beads for the remediation of Cr(VI) contaminated waters. Environ. Pollut. 214, 419–429. doi:10.1016/j.envpol.2016.04.034

Toli A., Alexopoulou M, Mystrioti Ch, A. Xenidis A, Papassiopi N., 2016b. Column tests for evaluating the remediation of Cr(VI) contaminated waters using resin supported nanoiron. Presented in the 13th International Conference on Protection and Restoration of the Environment, 3rd to 8th July, 2016 | Mykonos island, Greece.

Tseng, H.H., Su, J.G., Liang, C., 2011. Synthesis of granular activated carbon/zero valent iron composites for simultaneous adsorption/dechlorination of trichloroethylene. J. Hazard. Mater. 192, 500–506. doi:10.1016/j.jhazmat.2011.05.047